Reviewer's comments are in black, and responses are in blue.

The impacts of three secondary ice production (SIP) processes on the electrification were evaluated by the mesoscale simulation. A new electrical model was constructed based on the fast spectral bin microphysics (SBM) scheme, which constitutes a significant contribution of this paper. This electrical model will serve as an effective tool for studying electrification and discharge processes. However, there are several key issues in the paper that require further clarification. Substantial revisions may be necessary to strengthen the supporting evidence. Specifically, the following matters should be considered:

Reply: We appreciate your insightful comments. The paper has been revised accordingly and has been improved a lot. Please see our responses below.

1. In the model validation section, it is recommended that the author can display a two-dimensional distribution of observed and simulated lightning activities. The entire inner domain is too large to effectively reflect the distribution of simulated lightning activity.

Response: Thank you for your comment. The two-dimensional distribution of observed and simulated lightning activities is shown in Fig. R1 and added in the revised paper. The location of lightning is consistent with low brightness temperature. In the model, we failed to simulate the convective cell between 30°N and 32°N, the modeled reflectivity in this area is lower than the observed. While for the southern convective cell, the simulations are consistent with observation. According to another reviewer's comments, a fourth secondary ice production mechanism by ice sublimational breakup has been added to our model (Deshmukh et al., 2022; Waman et al., 2022). The experiment with all four SIP processes included is named "4SIP", and that with ice sublimational breakup only is named "SK".

Reference:

Deshmukh, A., Phillips, V. T. J., Bansemer, A., Patade, S. and Waman, D.: New Empirical Formulation for the Sublimational Breakup of Graupel and Dendritic Snow, J. Atmos. Sci., 79(1), 317–336, doi:10.1175/JAS-D-20-0275.1, 2022.

Waman, D., Patade, S., Jadav, A., Deshmukh, A., Gupta, A. K., Phillips, V. T. J., Bansemer, A. and Demott, P. J.: Dependencies of Four Mechanisms of Secondary

Ice Production on Cloud-Top Temperature in a Continental Convective Storm, J. Atmos. Sci., 79(12), 3375–3404, doi:10.1175/JAS-D-21-0278.1, 2022.

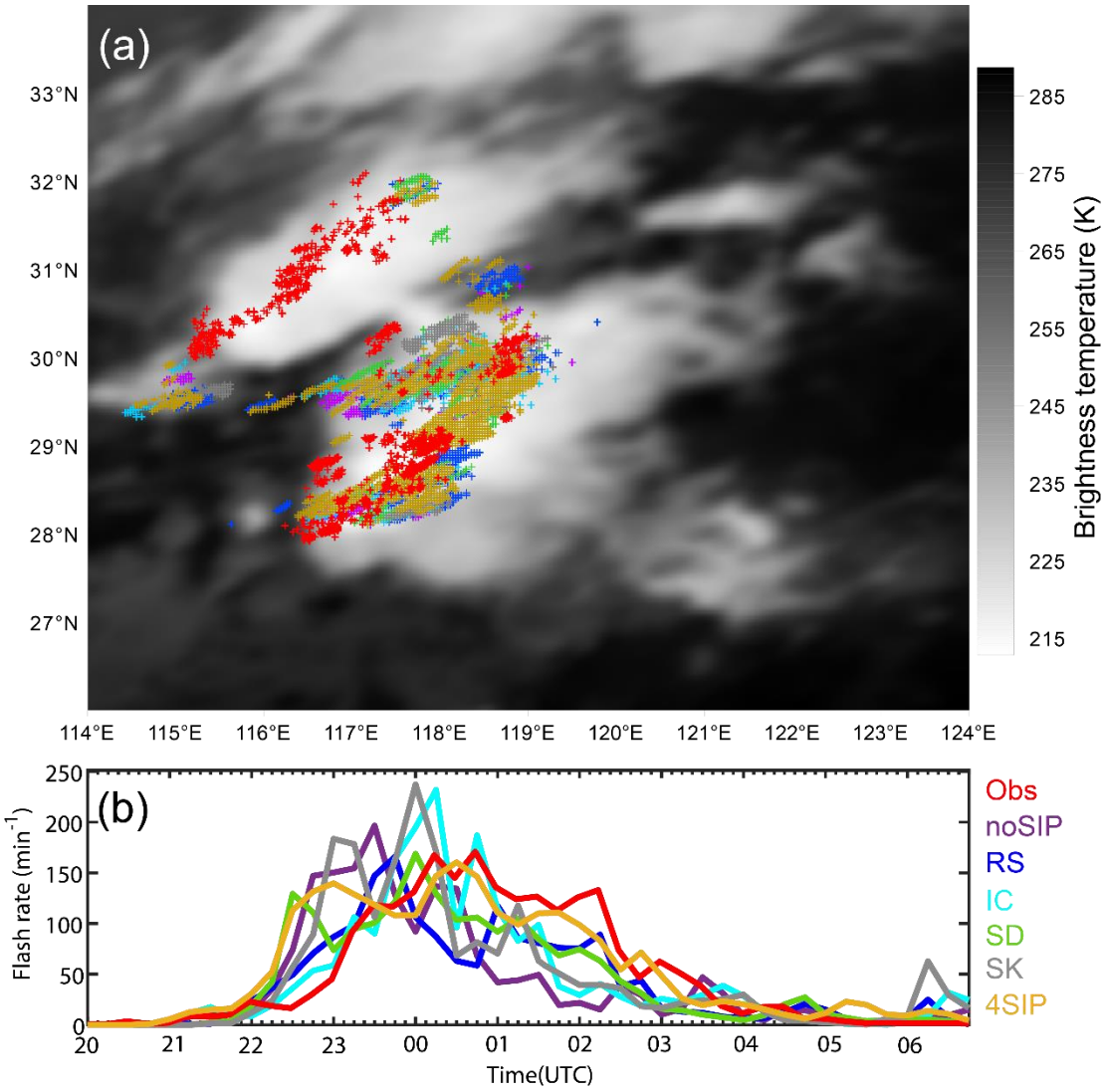

Figure R1. The (a) lightning location, and (b) time series of flash rate from observation and the six numerical experiments.

2. How was Figure 7 (as well as all time-height diagrams) created? Does Figure 7 present single-point data or regional average data? If it is regional average data, is it an average of the entire inner domain? Time-height diagrams for single-point or regional average data may better display the changing trends of variables, while cross sections can provide a more intuitive understanding. Cross sections for charging rates could also be shown.

Response: We appreciate the comment, and sorry for not explaining clearly. In the original paper, Figure 7 shows an average of the entire inner domain. In the revised

paper, we average only in-cloud regions. The cross sections of mixing ratio and number concentration of graupel, snow, and rain are shown in Fig. R2 and R3, and the cross sections of charge density on graupel and noninductive charging rate are shown in Fig. R4. These figures help understand the spatial distribution of microphysics and electrification. It is seen that though the impact of the ice-ice collisional breakup is small on average (which is seen in the time-height diagrams), this process can significantly enhance graupel or ice concentration in some areas (Fig. R2c, i, o). It is difficult to tell which SIP process has the most significant impact on cloud microphysics simply based on these cross sections, as the composite impact of the four SIP processes is not simply a sum of them (Fig. R2f, l, r, x). But according to the time-height diagrams, on average, the rime-splintering has a stronger impact on the cloud microphysics and electrification (Fig. R6)

The charge separation is found in areas with relatively high graupel and ice concentration. All four SIP processes, especially the rime-splintering process, can enhance positive charge separation at low levels. In addition, the ice-ice collisional breakup can enhance negative charging rates at high levels. The graupel charge density in the 4SIP experiment is more similar to that in the RS experiment. These cross-sections also help to understand the substantial difference between the charge density and charging rate, which is related to comment 3 (please see reply to comment 3.)

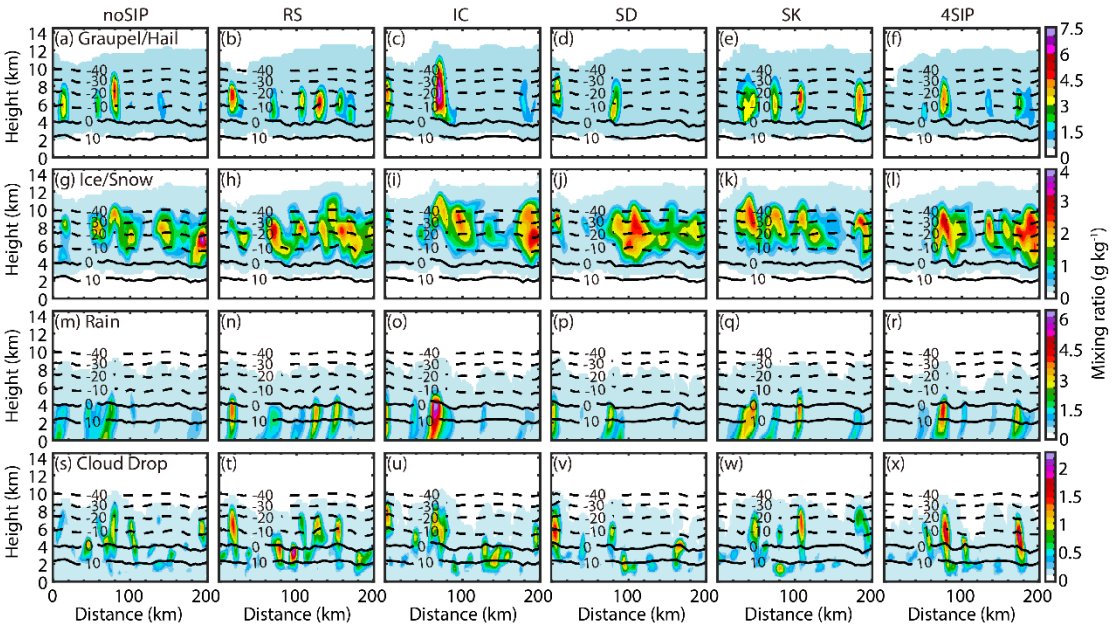

Figure R2: Cross sections of the modeled mixing ratio for (a)-(f) graupel/hail, (g)-(l) snow/ice, (m)-(r) rain and (s)-(x) cloud droplet at 01:00, Nov. 28th.

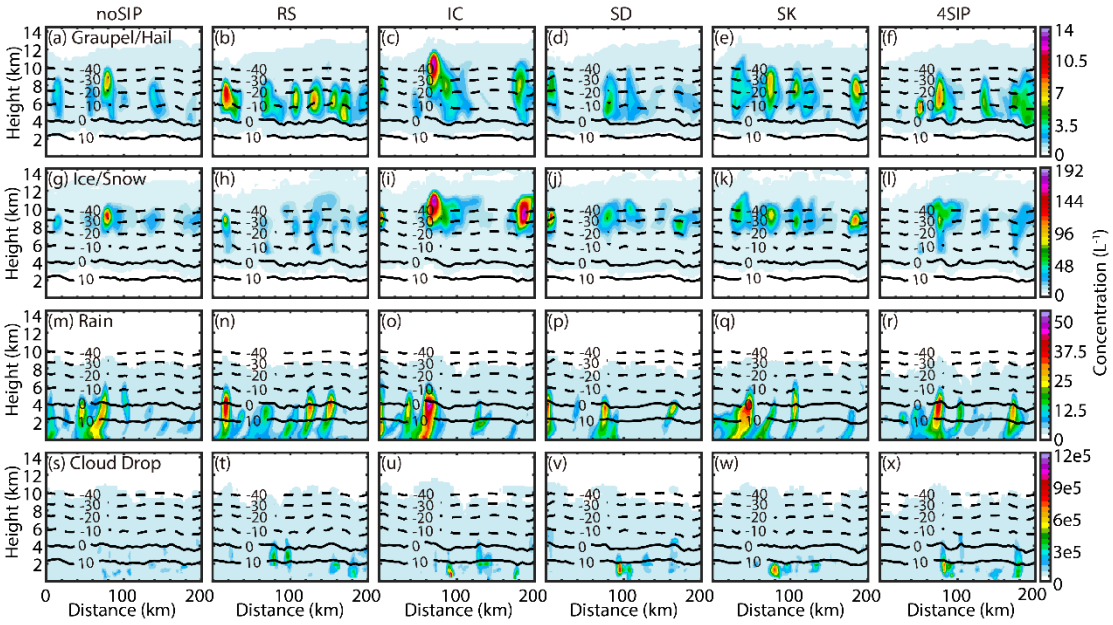

Figure R3: The same as Fig. R2 but for concentration.

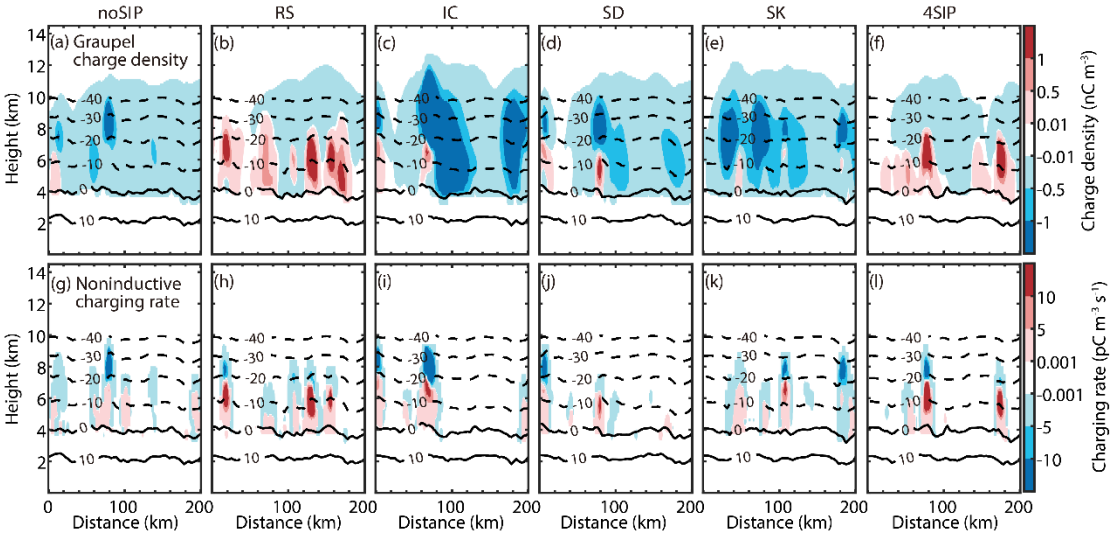

Figure R4: Cross sections of the modeled (a-f) graupel charge density and (g-l) noninductive charging rate at 01:00, Nov. 28th.

3. The correlation between charge structure and electrification rate does not align. Based on the charging rate distribution presented in Figure 9, it is observed that although the inductive charging rate varies significantly across different experiments, the non-inductive charging rate is one order of magnitude higher than the inductive charging rate. Therefore, we continue to lean towards the notion that electrification in the cloud is primarily attributed to the non-inductive collision process. However, it is noteworthy that even when there is a minimal difference in the non-inductive

electrification rate (Fig. 9 a, c, e, g, i), it leads to completely distinct charge distributions (Fig. 10), which is indeed perplexing. If our understanding is correct, the non-inductive charging rate depicted in Figure 9 should be targeted at graupel particles. Given this distribution, it should not cause such a considerable difference in electrification as observed in Figure 10. However, the substantial difference is difficult to explain solely by the sedimentation of graupel particles. Is it possible that the regional average has concealed some crucial information? Or we suspect that the inductive charging process may also play a vital role in the formation of charge structure. Therefore, it is suggested that the effects of inductive and non-inductive electrification should be separated.

Response: Thank you for your professional comment. According to your comment, we made a sensitivity test in which only noninductive electrification is used. Figure 5R shows the graupel charge density, noninductive charging rate, and the fraction of area with charge separation occurring. In the noSIP experiment, the graupel charge density is negative, while the noninductive charging rate has a bipolar structure. The magnitude of the low-level positive charging rate is much smaller than the high-level negative charging rate. This result is the same as that shown in the original paper, in which both noninductive and inductive charging are considered. Therefore, it is evident that the charge density is mainly controlled by noninductive charging. The different structures of the average charge density and charging rate indicate some crucial information is canceled by averaging. Since a threshold of RAR>0.1 g m^{-3} s^{-1} is required to trigger charge separation, charging takes place only in a small fraction of the cloud area (Fig. R5e and f). This is more intuitive in the cross sections shown in Fig. R4. Charging only occurs in areas with relatively high graupel concentration (Figs. R4g-l and R3), while fall of graupel with negative charge is found in more areas. If the magnitude of the low-level positive charging rate is small, the average charge density would be negative, while if the magnitude of the low-level positive charging rate is enhanced by SIP, the average low-level charge density on graupel is positive. This information is added to the paper.

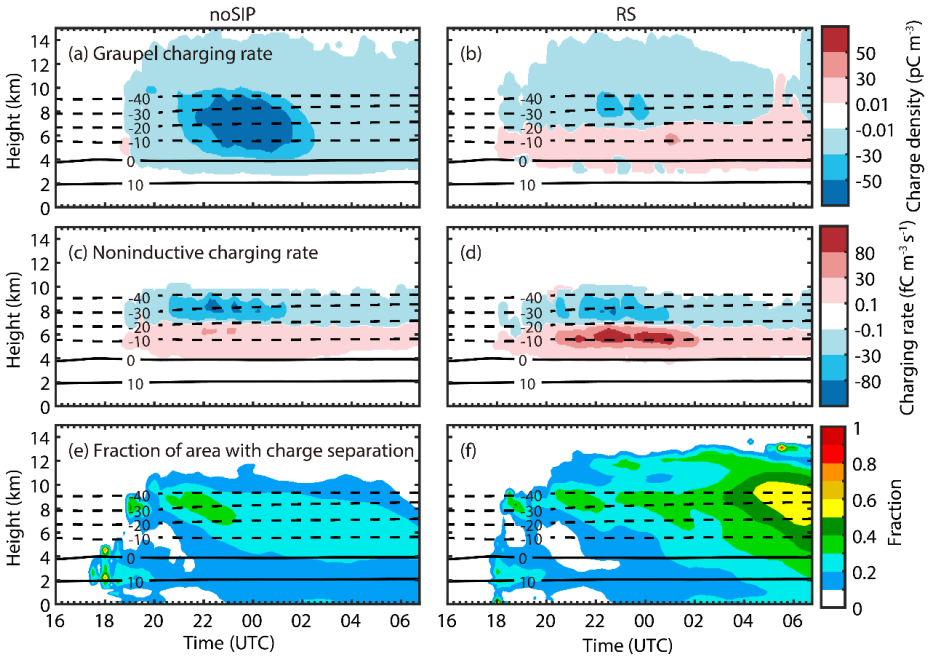

Figure R5. Time height diagrams of (a, b) graupel charge density, (c, d) noninductive charging rate, and (e, f) fraction of area with charge separation occurring in noSIP and RS experiments with only noninductive charging used.

4. The rationale for the charge structure differences in various experiments is not clear. Although the author demonstrated the differences in charge structure caused by different SIP processes, we believe that the underlying reason has not been fully disclosed. When the SIP process changes, what is the fundamental alteration? Which leads to the change in electrification rate and charge structure? Has the rime accretion rate (RAR) changed significantly? What causes the change in RAR?

Response: Thank you for your professional comment. The most significant change in charge structure is the low-level positive charge is enhanced, especially by RS. This can be interpreted based on the equation of non-inductive charging produced during the collision between graupel and ice crystal:

$$\frac{\partial \rho_{gi}}{\partial t} = \iint_0^\infty \frac{\pi}{4} \beta \delta q_{gi} (1 - E_{gi}) |V_g - V_i| (D_g + D_i)^2 n_g n_i dD_g dD_i$$

Based on this equation, we can see the charge transfer is determined by three terms: 1) charge transferred during each collision between graupel and ice (δq_{gi}); 2) collision kernel between graupel and ice; 3) concentration of graupel and ice. δq_{gi} is determined by RAR, which is a function of liquid water content (LWC) and terminal velocity of graupel. With the addition of SIP, the LWC generally decreases (Fig. R6),

and the diameters of ice particles decrease too, leading to a decrease in RAR (Fig. R7), especially in RS and SD experiments. The collision kernel between graupel and ice is determined by the terminal velocity and sizes of graupel and ice, which also decreases after SIP processes are implemented. The concentrations of graupel (n_g) and ice (n_i) increase due to the RS and SD processes, this explains the enhanced low-level charging by these two processes. This is added in the discussion section.

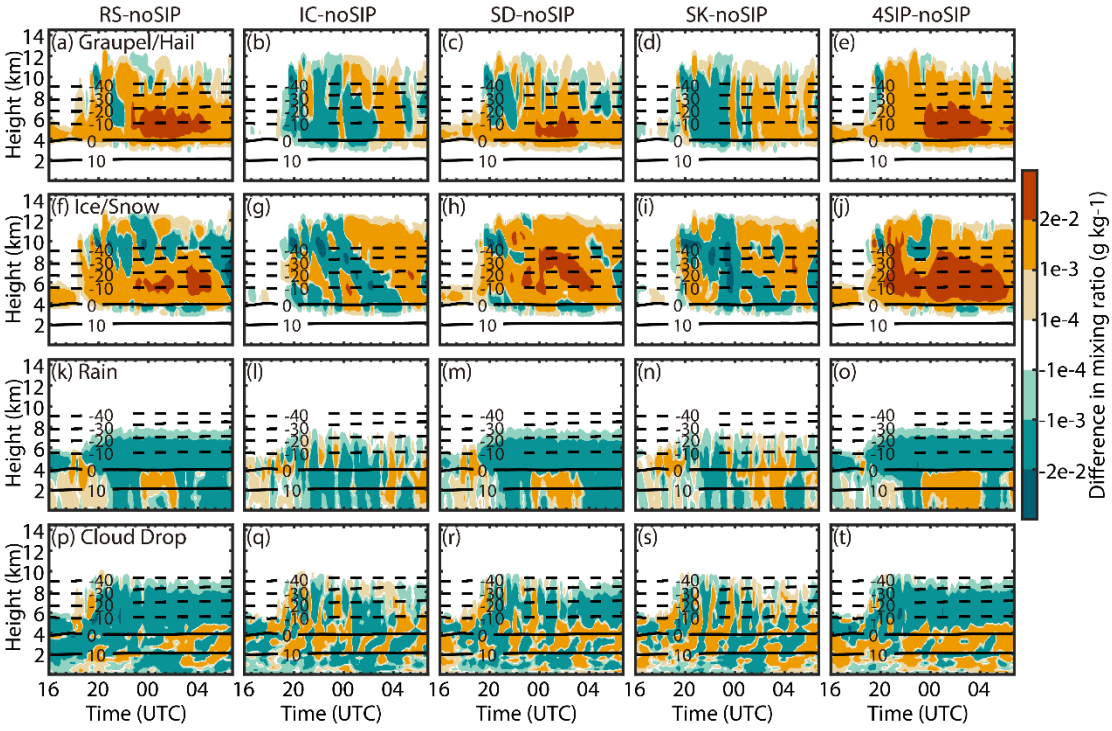

Figure R6. Difference in mixing ratio of (a-e) graupel/hail, (f-j) ice/snow, (k-o) rain and (p-t) cloud droplets between the experiments with SIP and that without SIP.

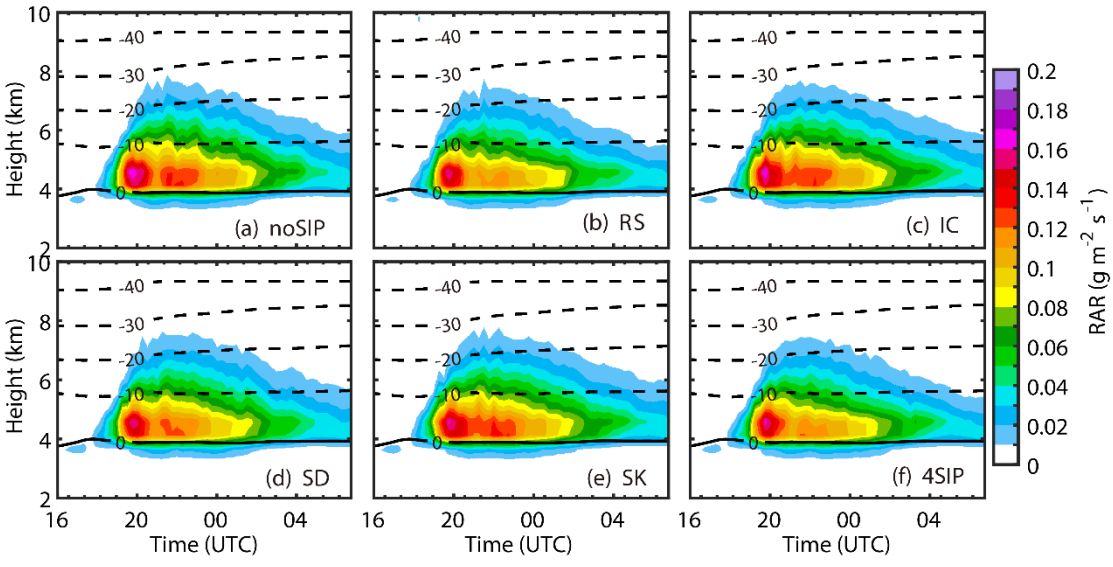

Figure R7: The time height averaged diagram of RAR. (a) experiment without SIP, (b)

experiment with rime-splintering (RS), (c) experiment with ice-ice collisional breakup (IC), (d) experiment with shattering of freezing drops (SD), (e) experiment with sublimational breakup (SK) and (f) experiment with four SIP processes.

5. The author should illustrate the specific location of the cross-sections in Figure 12 within Figure 5.

Response: Sorry for not explain clearly. The location of the cross-sections is illustrated in the revised figure now (black line in Fig. R8a).

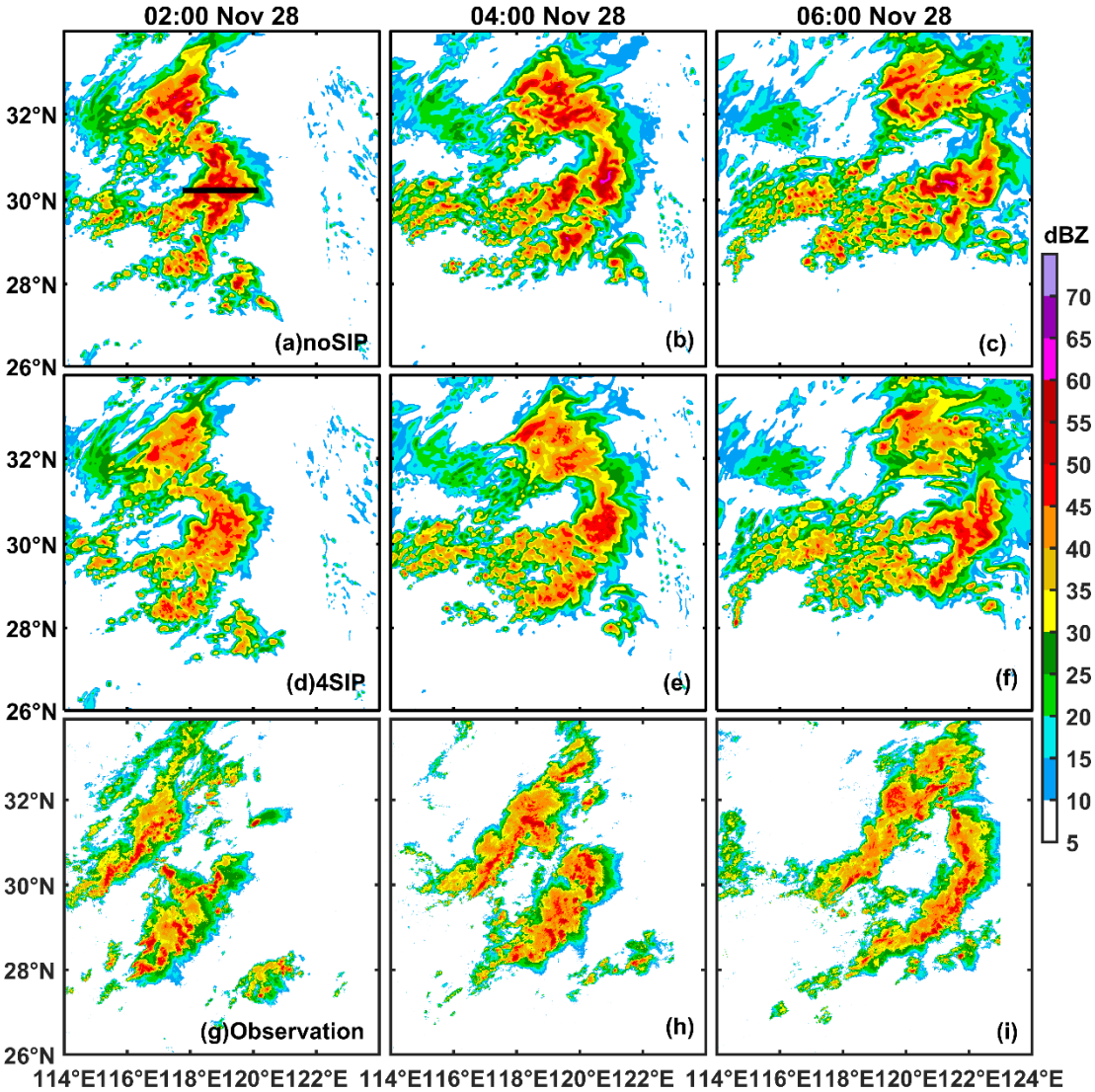

Figure R8. Composite radar reflectivity from (a-c) noSIP, (d-f) 4SIP experiment, and (g-i) observation at 02:00, 04:00, and 06:00, Nov 28th.